Title: Influence of milling time on formation of NiTi alloy produced by high-energy ball milling

Author: Piotr Salwa, Tomasz Goryczka

P. SALWA*#, T. GORYCZKA*

INFLUENCE OF MILLING TIME ON FORMATION OF NiTi ALLOY PRODUCED BY HIGH-ENERGY BALL MILLING

Mixture of nickel and titanium powders were milled in planetary mill under argon atmosphere for 100 hours at room temperature. Every 10 hours the structure, morphology and chemical composition was studied by X-ray diffraction method (XRD), scanning electron microscope (SEM) as well as electron transmission microscope (TEM). Analysis revealed that elongation of milling time caused alloying of the elements. After 100 hours of milling the powders was in nanocrystalline and an amorphous state. Also extending of milling time affected the crystal size and microstrains of the alloying elements as well as the newly formed alloy. Crystallization of amorphous alloys proceeds above 600°C. In consequence, the alloy (at room temperature) consisted of mixture of the B2 parent phase and a small amount of the B19' martensite. Dependently on the milling time and followed crystallization the NiTi alloy can be received in a form of the powder with average crystallite size from 1,5 up to 4 nm.

Keywords: NiTi alloys, high-energy ball milling, crystallite size, microstrain, lattice parameters

1. Introduction

The size of the grain had a significant impact on the course of martensitic transformation. Especially, this effect can be visible in the NiTi alloys, where the grain size was reduced previously down to micro-meters [1] and recently even to a few nanometers [2,3]. Possibility to obtain shape memory effects, in the case of nanocrystalline grains, increased interest and adoption of methods for obtaining NiTi alloys with significantly reduced size. For this purpose, methods used for amorphization and/or nanocrystalization have been adopted with combination of heat treatment. Amorphization of the NiTi alloys can be realized via cold rolling [4], ion implantation [5], electron irradiation [6], rapid solidification [7] sever plastic deformation [8] or mechanical alloying [9-11].

However, the methods related to mechanical alloying through high energy grinding deserve particular attention [12-14]. Adjustment of parameters such as grinding time and speed of the grinder allow obtaining alloy with a crystallite size less than 10 nm. In this work, a comprehensive analysis of the structure done for alloying elements and the NiTi alloy was carried out. The obtained results, supported by research from two independent methods, confirmed the possibility of creating a homogeneous NiTi alloy with a crystallite size lower than 4 nm.

2. Materials and methods

Commercial nickel and titanium elemental powders (Atlantic Equipment Engineers) of 99.7% purity and average particle size of 4-8 μm and 20 μm, respectively, were used for production of NiTi alloy with equiatomic nominal chemical composition. First, proper weight of powders was mixed by 48 hours in the Netzsh planetary mill. This mixing step leads to better distribution of the mixed components in the entire volume and limits the formation of their agglomerates. Next, alloying of the elements was done by milling in high-energy Fritsch Pulverisette 7 premium line planetary-ball mill at argon protective atmosphere for 100 hours. The process was carried out with 250 rpm milling speed and the weight ratio of the balls to the material was 10:1. Every 10 hours, a portion of milled powder was collected and subjected to structural and morphological studies.

Structure of mixture was examined by X-ray diffraction technique (XRD) using X'Pert-PRO diffractometer with copper radiation ($CuK_{\alpha1\,and\,2}$). The X-ray diffraction patterns were measured in step-scan mode and a range of 2θ: 10-140° with step 0.04° and time adjusted to obtain the appropriate counting statistics. Phase analysis was done using the ICCD PDF-4 database.

Morphology of mixed powders was observed using scanning electron microscope JEOL JSM6840 (SEM) equipped with and X-ray energy dispersive spectrometer (EDS). Average particle size for initial and mixed powders was determined from measurement done with use the Coulter Laser Scattering Particles Size Analyzer (CLSPSA).

Structure in nano-scale was studied using an transmission electron microscope JEOL 3010 operated at 300 kV. Samples for TEM observations were submersed in an isopropyl alcohol and ultrasonicated for 30 min, then deposited on carbon coated grid and dried.

* UNIVERSITY OF SILESIA IN KATOWICE, INSTITUTE OF MATERIALS SCIENCE, 1A 75 PULKU PIECHOTY STR., 41-500 CHORZOW, POLAND

Corresponding author: salwa.piotr@gmail.com

Crystallization of the alloy was carried out inside the Mettler Toledo DSC 1 calorimeter, heating the sample to 600°C in an argon protective atmosphere.

3. Results and discussion

The morphology of the titanium and nickel powders was changing at various stages of NiTi alloy production. Powder of nickel, in its initial state, had the shape of jagged ovals (Fig. 1a) while titanium was in the form of irregularly shaped blocks (Fig. 1b). The average particle size was 11 μm and 35 μm for nickel and titanium, respectively. After homogenizing mixing in a planetary mill, nickel and titanium showed rounded shapes (Fig. 1c). In some places, mechanically connected particles of both elements were observed. Moreover, free mixing caused a slight reduction in the average size of powders down to 7 μm and 30 μm for nickel and titanium, respectively.

The most important part of the procedure, leading to obtaining the alloy, was the use of high-energy ball milling. After 10 hours of mixing, the particles joined and formed agglomerates with an average size of about 112 μm (Fig. 1d). These agglomerates had regular shapes and were close in size. They were created in result of mechanical joining of powder particles. This effect was visible on the distribution maps of alloying elements (Fig. 2a), where clearly separated areas of nickel and titanium appeared. Increasing the grinding time to 60 hours caused that the greater part of large agglomerates has been fragmented into particles with an average size lower than 80 μm. However, a few agglomerates with size over 200 μm were still observed
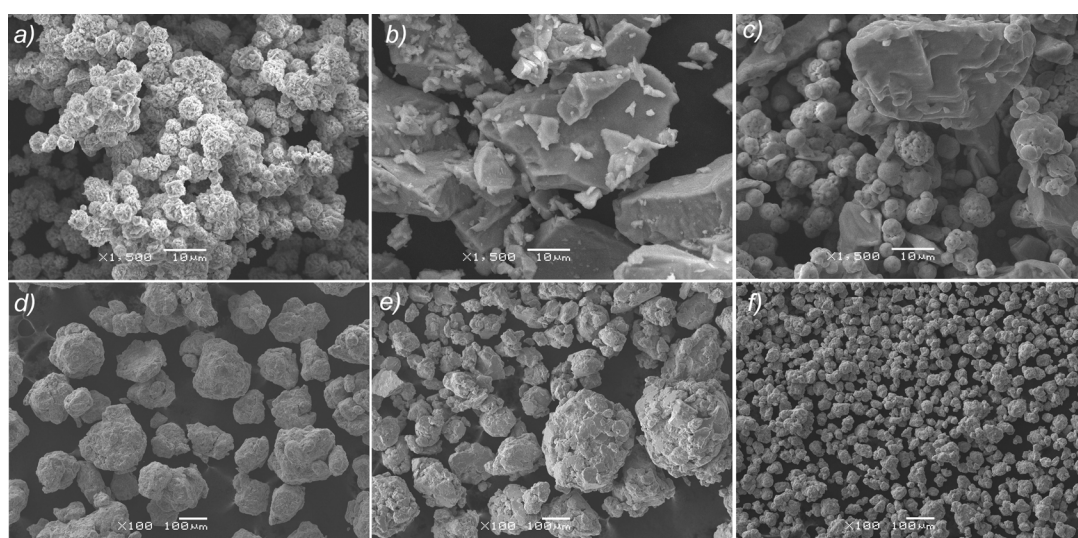

Fig. 1. SEM images observed for powders: a) nickel, b) titanium, c) mixture after 48 hours of homogenization, and after high energy ball milling d) 20 hrs, e) 60 hrs, f) 100 hrs
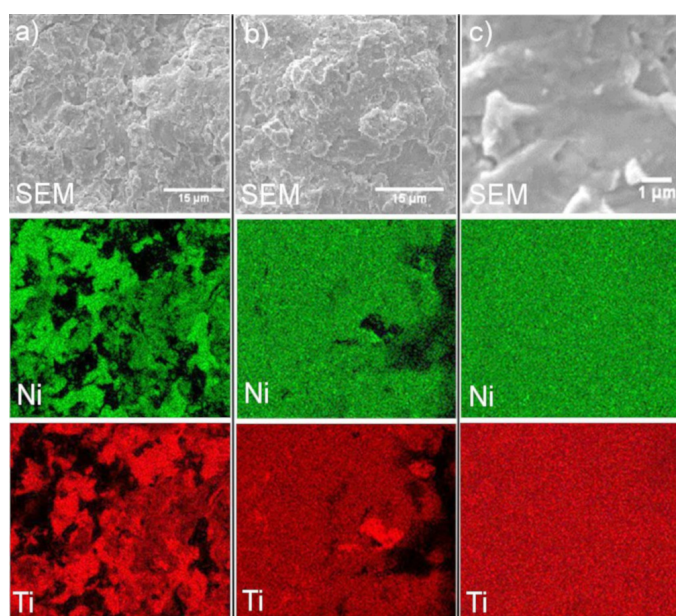

Fig. 2. SEM image and distribution map of alloying elements after milling time: a) 20 hrs, b) 60 hrs, c) 100 hrs

(Fig. 1e). After 60 hours of milling, the distribution of alloying elements inside in the particles was different from that observed after 10 hours of grinding. The distribution map of the elements shows evidently that the previously visible boundaries of the elemental particles begin to disappear and the concentration of elements begins to equalize throughout the particle (Fig. 2b). However, in some places an increased concentration of titanium still existed. This effect could come from the larger size of the titanium powder and difficulty with their granulation. A further increase of the grinding time to 100 hours led to homogenization of both: the shape of the particles and their size (Fig. 1f). The globular particles were sized about 75 μm. Distribution maps of elements, reveal the even distribution of alloying elements in the particles (Fig. 2c).

The influence of milling time on structural changes was studied with application of X-ray diffraction methods. The selected measured diffractograms are shown in Fig. 3. The free mixing of the powders for 48 hours did not bring any significant changes to phase composition of the mixture (Fig. 3a). The measured diffraction lines were identified as belonging to
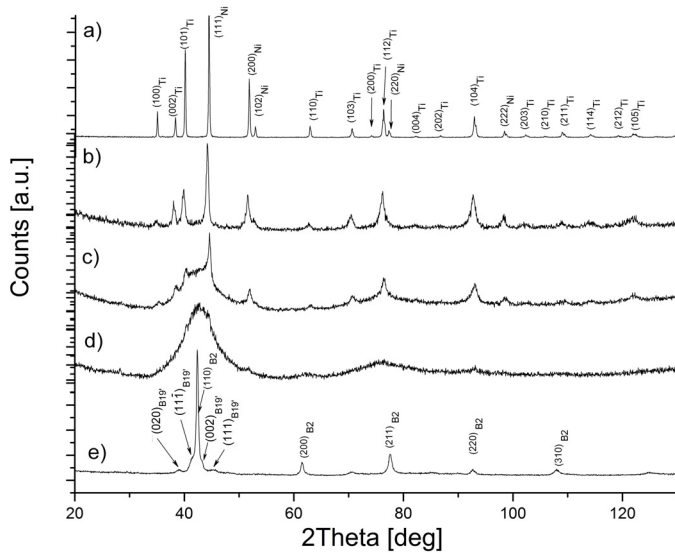
Fig. 3 X-ray diffraction patterns of powders at various stages of: mixed for 48 hrs (a); high-energy milling: 20 hrs (b), 60 hrs (c), 100 hrs (d) and after crystallization at 600°C (e)

nickel and titanium (PDF-4 card no. 00-004-0850 and 00-044-1294, respectively). However, the high-energy milling yielded structural and phase changes of the mixed powders. First of all, as the milling time is extended, the phase composition has changed. Generally, the amount of titanium and nickel, that had been alloyed, was reduced as grinding time progressed. Already after 20 hours of milling, the elements began to diffuse into each other forming a NiTi alloy (Fig. 3b). The evidence for this was the lowering of the Ni and Ti diffraction lines intensities and simultaneously appearance of broaden peak at 2θ position about 42,5 degrees. The intensity of this peak increased as the grinding time increased whereas the intensity of the peaks, coming from nickel and titanium, decreased gradually (Fig. 3c). After 100 hours of high energy milling, mainly two intense and broaden peaks, in the 2θ positions of 42.77^{o} and 76.47^{o} and respectively half-width of 6.7^{o} and 10.2^{o}, were visible (Fig. 3d).

Depending on the temperature range, the binary NiTi alloy may reveal the presence of the B2 parent phase and/or the martensite B19'. Increasing the share of nickel and/or presence of the internal, local stresses may result in appearance of additional phase: the R-phase [15-17]. In order to determine the phase composition of the created alloy, in the micro-, nano-scale and to adopt the structure model for calculations, microscopic observations were carried out (Fig. 4). After 20 hours of grinding, TEM images confirmed the presence of finely divided nickel and titanium nano-particles (Fig. 4a left image) as well as the nano-particles of the NiTi alloy – the precursor of B2 parent phase (Fig. 4a right image). The structure of the crystalline B2 parent
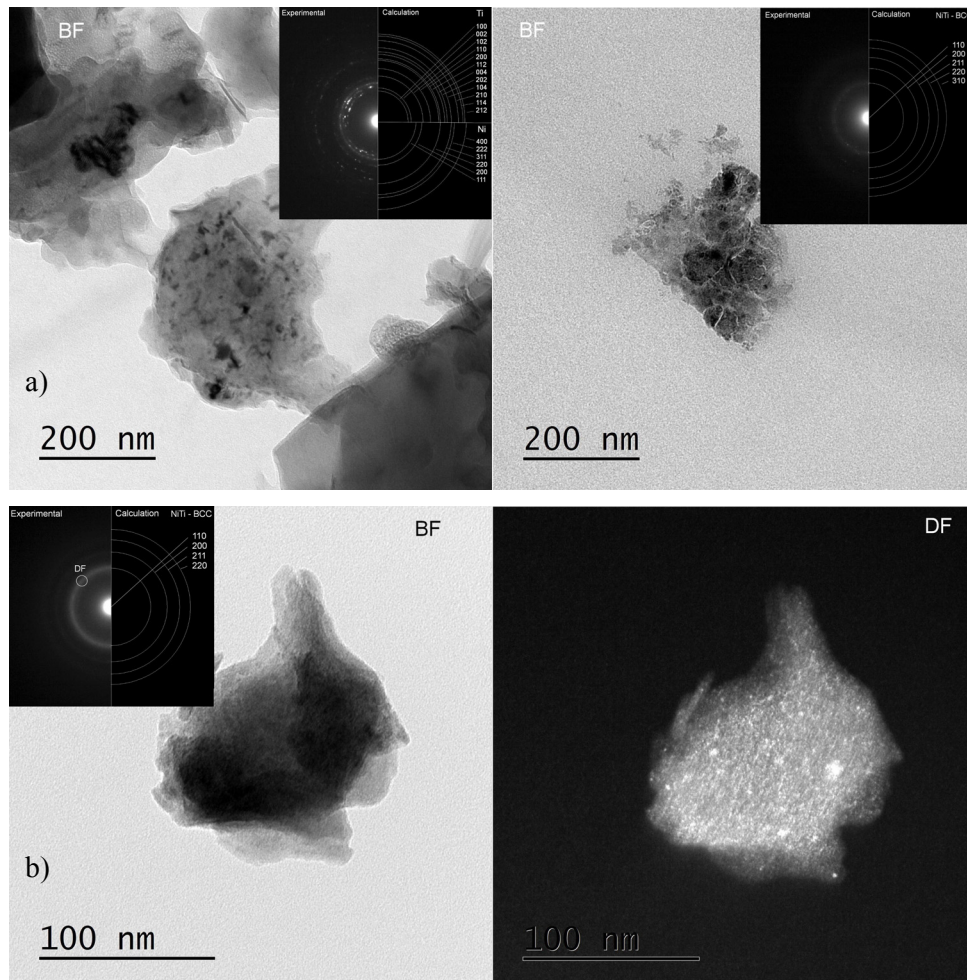

Fig. 4. TEM images (bright field – BF and dark field – DF) as well as SAED patterns observed for the powders milled after 20 hrs (a) and 100 hrs (b)

phase is described as ordered one with a crystal lattice of body cubic centered – CsCl type. In this case, in addition to the fundamental peaks, diffraction images (XRD, electron diffraction) show, the presence of the superlattice peaks or spots. In the case of presented results, obtained after different grinding times, the diffraction effects coming from the presence of the superlattice were not observed. For the sake of clarity of the article, it was assumed that the nano-crystalline particles of the NiTi alloy are formed as disordered body cubic centered phase – precursor of the B2 phase. Consequently, this phase was marked as the BCC one. In general, the amount of the BCC phase increased as the mixing time increased. After 100 hours of grinding – only the presence of the BCC phase was stated (Fig. 4b). Contrary to the results published at [10], the presence of the B19' martensite was not stated. Samples for microscopic examination were prepared from powder weighing about a dozen milligrams. Hence, it was impossible to omit the eventual presence of the martensite or the R-phase. Therefore, for further calculations, it was assumed that the powder at the milling stages consists of titanium, nickel and finally NiTi alloy with the structure of the BCC phase.

In order to investigate the effect of grinding time on the structure of alloy elements and the formed alloy, the X-ray diffractograms were fitted using the Rietveld method [18]. From these calculations, the values of the lattice parameters and the half widths (FWHM) were received. Further, the values of the FWHM of the diffraction peaks were used to calculate the crystallite size and internal stresses. In this case the Williamson-Hall method was applied [19]. Figure 5 shows the impact of grinding time on the change of lattice parameters. In the case of alloying elements, the values of the lattice parameters increased until the grinding time was 50-60 hours. In this interval, the lattice parameters of the BCC phase remained almost unchanged. After extending the grinding time over 60 hours, the values of lattice parameters for both alloying components as well as the the BCC phase rapidly began to decrease. This trend is in line with the trend of the impact of grinding time on the increase in the microstrains of both alloying components (Fig. 6). After 60 hours of milling, the values of microstrains decrease, so in the case of nickel (after 80 hours) it changed to negative one. It means that, contraction of the crystallographic lattice appeared. Such behaviors and trends can be explained as follows. During the first hours of mixing, colliding balls with powder particles cause that the powder clumps into larger agglomerates. It is worthy to remind that a rise in the average size of agglomerates was observed in SEM images (Fig. 2d-e). The supplied energy acts as in the traditional and sever deformation of the NiTi alloy, increasing the quantity and the density of structural defects. First of all, the density of dislocations increases, low-angle grains boundary as well as stacking faults are created [20-23]. In addition, the energy is used to drive atoms from one alloying element into the other. It results in increase of the crystal lattice parameters as well as lattice strain. Further increase of energy, supplied by increasing the grinding time over 60 hours, is used for formation of grain boundaries. As a result, average grain size is refined. Moreover, this energy and the temperature facilitate the diffusion

of alloying elements to the newly formed alloy. Thus shrinkage or contraction of the local crystal lattice can be expected. At the same time, an intense increase in the amount of the BCC phase was observed. Also, extending of the grinding time over 60 hours took effect also on the newly formed alloy. In the mechanically deformed the BCC phase, done by collision with the balls, the lattice parameter reduced to 2.993 [Å] (Fig. 5b).
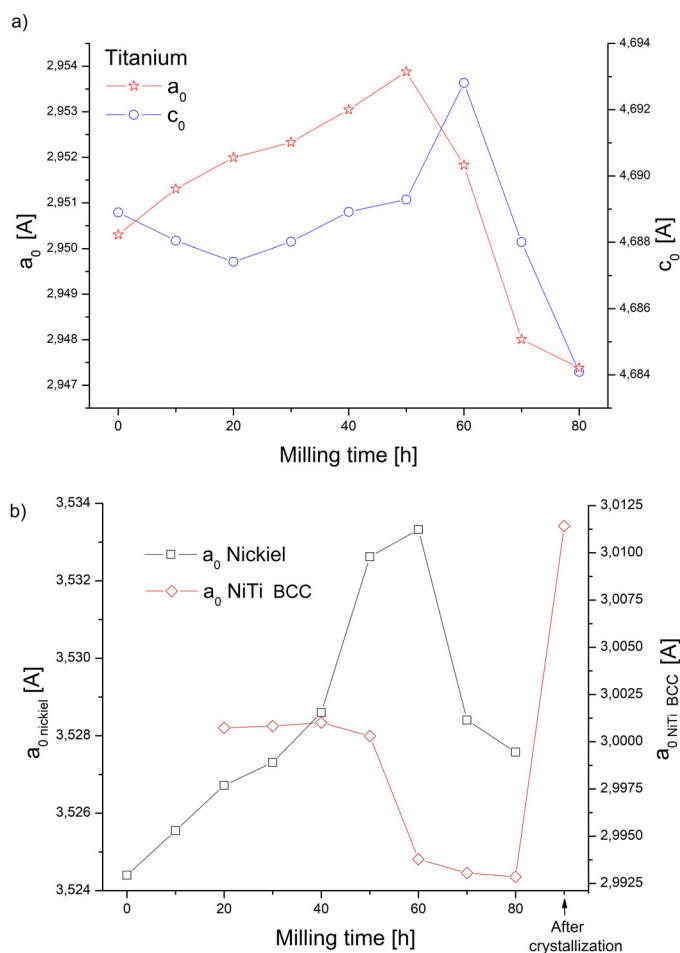

Fig. 5. Calculated lattice parameters versus high-energy milling time for: titanium (a), nickel and the BCC phase (b)

The effect of the grinding conditions is the change in the average size of the crystallites for both alloying elements and the BCC phase. The size of the alloying elements decreases with increase of the milling time (Fig. 6). The significant change in crystallite size occurs between 10 and 30 hours. In the case of nickel, this is a decrease from about 160 nm to about 30, while the size of the titanium crystallites decreases from about 60 nm to about 24 nm. Extending the grinding time has a weaker influence on the crystallite size. After 100 hours, the size of nickel crystallites reaches about 20 nm, and titanium about 10 nm. Received results are in a good agreement with one obtained by Arunkumar et al. [24].

In the case of the crystal size determination of the BCC phase, the use of the Williamson-Hall method basing on X-ray experiments is useless due to its limitations. This limitation comes from the difficulty of separation of FWHM part, which
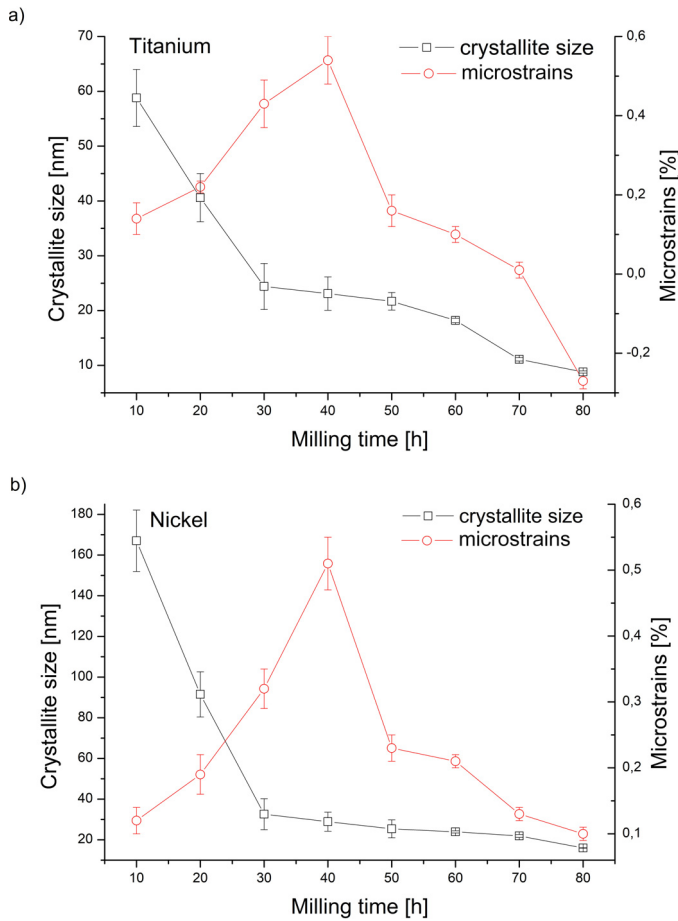
a)

b)

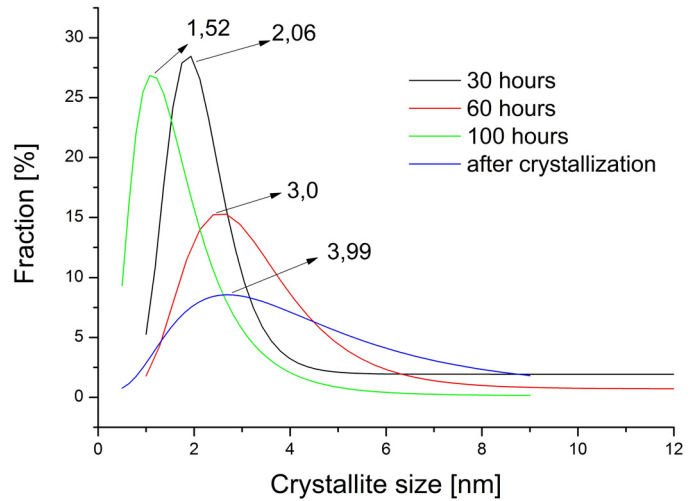Fig. 6. Crystallite size and microstrains versus milling time for: titanium (a) and nickel (b)

Fig. 7. Comparison of fitted lognormal function determined from histograms for the BCC phase after various milling times and crystallization

was determined on the basis of DF images analysis using the computer program ImageJ [25]. The obtained distributions of the crystallite size were fitted with use of the lognormal function. The average crystallite size was determined from the maximum of the distribution. Received results were shown in Fig. 7. The BCC phase is formed after 20 hours of grinding. The average size of crystallites, after 30 hours, was 2 nm. Extending the grinding time to 60 hours resulted in an increase in the average size up to 3 nm. Further milling resulted in a reduction of the average size to 1.5 nm. A part of the alloy occurred in the form of an amorphous phase. Presence of this phase was confirmed by scattered rings observed on electron diffraction patterns. Thus, the alloy after 100 hours of grinding was subjected to the crystallization inside the calorimeter. The sample was heated to 600°C at a rate of 20 deg/min. The X-ray diffraction pattern, fitted with Rietveld method, shows that at room temperature alloy consists of the B2 parent phase and a small amount of the B19' martensite (Fig. 8). Result were confirmed from TEM observation (Fig. 9). Determined lattice parameters for the B2 phase was

comes from the amorphous phase from that coming from the sub nanocrystalline one. As mentioned before, the half-widths determined for peaks exceed 6 degrees. Such values are characteristic of an amorphous and/or sub nanocrystalline material (size lower than 4-5 nm). In contrast to [10], the size of the parent phase crystals was determined from microscopic observations using the dark field technique (Fig 4). The average size
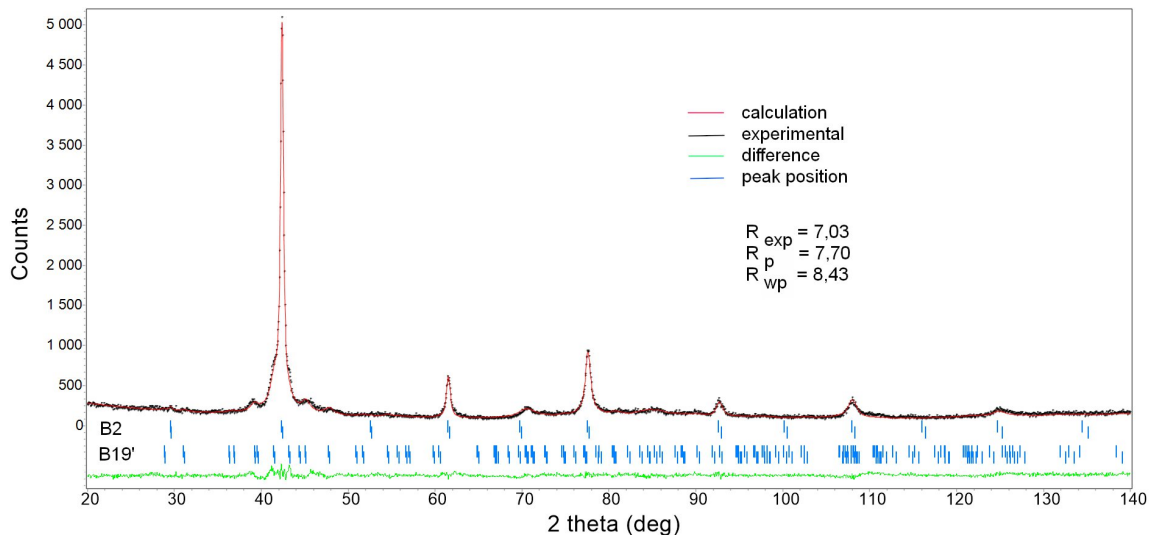

Fig. 8. Results of the Rietveld refinement for NiTi alloy after crystallization at 600°C
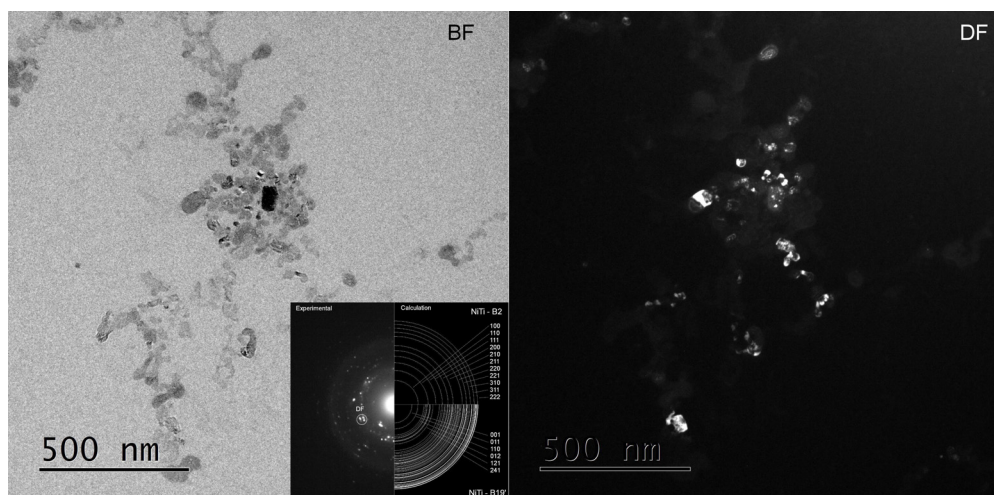
Fig. 9. TEM images (bright field BF and dark field DF) as well as SAED patterns observed for the powders after crystallization at 600°C

3.0122 Å, whereas for the martensite as follows: $a_0 = 2.8527$ Å; $b_0 = 4.5810$ Å; $c_0 = 4.1926$ Å and $\gamma = 96.3°$. Received results are in a good agreement with these presented at [26]. The average crystal size of the B2 phase, which was about 4 nm, was also determined based on DF images.

4. Conclusions

- Mechanical alloying of equiatomic NiTi elemental powders leads to nano-crystallization of synthesized alloy. This process starts after 20 hours of milling and completes after 100 hours of milling.
- Distribution of alloying elements changed throughout whole milling time. After 100 hours of milling homogeneous distribution of nickel and titanium was received.
- Elongation of the milling time up to 60 hours causes increase of the crystal lattice parameters of alloying elements as well as microstrains.
- Milling with the time ranged from 60 to 100 hours influenced the grain refinement, decrease of the crystallites size and the crystal lattice contraction of the alloying elements and the BCC phase – precursor of the B2 parent phase.
- The average crystallite size determined for the crystallized NiTi powder increased to 4 nm.

REFERENCES

[1] F.J. Gil, J.M. Manero, J.A. Planell, J. Mat. Sci. **30**, 2526-2530 (1995).

[2] T. Waitz, V. Kazykhanov, H.P. Karnthaler, Acta Mat. **52**, 137-147 (2004).

[3] J. Ye, R.K. Mishra, A.R. Pelton, A.M. Minor, Acta Mat. **58**, 490-498 (2010).

[4] G.B. Cho, Y.H. Kim, S.G. Hur, Ch.A. Yu, T.H. Nam, Met. and Mat. Intern. **12**, 173-179 (2006).

[5] P. Moine, J.P. Rivieri, M.O. Ruault, J. Chaumont, A. Pelton, R. Sinclair, Nuc. Instr. Meth. in Phys. Research B **7-8**, 20-25 (1985).

[6] H. Mori, H. Fujita, Jap. J. Appl. Phys **21**, L494-L496 (1982).

[7] P. Vermaut, L. Lityńska, R. Portier, P. Ochin, J. Dutkiewicz, Mat. Chem. and Phys. **81**, 380-382 (2003).

[8] S. Jiang, L. Hu, Y. Zhang, Y. Liang, J. Non-Cryst. Solids **367**, 23-29 (2013).

[9] R.B. Schwarz, R.R. Petrich, C.K. Saw, J. Non-Cryst. Solids **76**, 281-302 (1985).

[10] E. Sakher, N. Loudjani, M. Benchiheub, M. Bououdina, J. Nanomat. (2018), DOI: 10.1155/2018/2560641.

[11] A. Takasaki, Phys Status Solidi A 169, 183-191 (1998).

[12] W. Maziarz, J. Dutkiewicz, J. Van Humbeeck, T. Czeppe, Mat. Sci Eng. A, 844-848 (2004).

[13] S. Khademzadeh, N. Parvin, P. Bariani, Int. J. Precis. Eng. Manuf. **16**, 2333-2338 (2015).

[14] M. Farvizi, Arch. Metall. Mater. **62**, 1075-1079 (2017).

[15] T. Saburi, T, Tatsumi, S, Nenno, J. de Phys. **43**, C4-261 (1982).

[16] M. Nishida, T. Honma, Scripta Met. **18**, 1293-1298 (1984).

[17] H. Morawiec, J. Ilczuk, D. Stróż, T. Goryczka, D. Chrobak, J. de Phys. IV **7**, C5-155-59 (1997).

[18] H.M. Rietveld, Acta Cryst. **22**, 146-151 (1967).

[19] C. Suranarayana, M.G. Norton, X-Ray Diffraction: A Practical Approach, Springer, New York (1998).

[20] L. Hu, S. Jiang, Y. Zhang, Y. Zhao, S. Liu, Ch. Zhao, Intermetall. **70**, 45-52 (2016).

[21] Y. Zhang, S. Jiang, L. Hu, Y, Liang, Mat. Sci. Eng. A **559**, 607-614 (2013).

[22] C. Rentenberger, T. Waitz, H.P. Karnthaler, Scripta Mat. **51**, 789-794 (2004).

[23] M. Zhu, M.Qi, A.Q. He, H.X. Sui, W.G. Liu, Acta Metall. Mat. **42**, 1893-1899 (1994).

[24] S. Arunkumar, P. Kumaravel, C. Velmurugan, V. Senthilkumar, Int. J. Min., Metall. Mat. **25**, 80-87 (2018).

[25] W.S. Rasband, ImageJ, U.S. National Institutes of Health, Bethesda, Maryland, USA, https://imagej.nih.gov/ij/, 1997-2018.

[26] J. Khalil-Allafi, W.W. Schmahl, H. Wagner, H. Sitepu, D.M. Toebbens, G. Eggeler, Mat. Sci. Eng. A **378**, 161-164 (2004).